Proceedings of the 2007 IEEE/RSJ International
Conference on Intelligent Robots and Systems
San Diego, CA, USA, Oct 29 - Nov 2, 2007

Designing Aerial Robot Sensor Suites to Account for Obscurants

Keith Sevcik and Paul Oh*
Drexel University, Philadelphia PA
Email: kws23@drexel.edu and paul@coe.drexel.edu

Abstract— **Recent events have proven the utility of aerial robots in search and rescue and military operations performed in near-Earth environments. However, autonomy in such environments is still limited by the robot's ability to perform collision avoidance. Real time, high fidelity maps can be utilized to assist the robot in performing collision avoidance. This paper explores the use of a laser range finder to accomplish real time map building in the presence of obscurants. Experiments were conducted to determine the probabilistic models of the sensor in the presence of rain and fog. These models are then utilized to map obstacles and terrain features in the presence of obscurants. Preliminary results show the implementation of these methods in an aerial vehicle testing facility.**

I. INTRODUCTION

Recent events have driven the need to develop robotic systems to assist in missions such as reconnaissance, search-and-rescue, and payload delivery. Towards these ends, the Drexel Autonomous Systems Lab is investigating the use of heterogeneous robotic teams comprised of unmanned ground vehicles (UGVs) and unmanned aerial vehicles (UAVs). UAVs provide an "eye in the sky", identifying points of interest and guiding UGVs operating on the ground.

The environments these robots encounter are rugged and hazardous for a human to traverse. Such near-Earth environments are challenging for robots, as well. GPS signals become degraded around tall buildings and trees. Obstacles such as rubble or wreckage would not show up on existing maps. UAVs provide a means around these shortcomings. An aerial vehicle flying through the scene can map the terrain, providing ingress and egress routes to operatives on the ground. This demands a sensor suite capable of detecting and mapping obstacles in near-Earth environments.

The design requirements for these sensors have been identified by the United States Defense Advanced Research Projects Agency (DARPA) and Future Combat Systems (FCS). The Organic Air Vehicle (OAV) and Class II programs both focused on building UAVs to fly missions in areas such as urban terrain and forests. A few fundamental requirements for sensor suites arose from these projects.

The range of the sensor must be chosen to give the craft time to perform collision avoidance. The required range and field of view scale with the flight speed and the dynamics of the vehicle. From previous experience detailed in [1], we found that most UAVs need at least 1 second to react.

*IEEE Member. Address all correspondence to this author. This work was supported in part by the National Science Foundation CAREER award IIS 0347430.

Fig. 1. Systems Integrated Sensor Test Rig (SISTR). SISTR permits real hardware to be tested in simulated urban environments and disaster scenarios. Environmental effects such as varied lighting, rain, and fog can be introduced in a controlled and repeatable fashion.

The sensor must also detect a wide range of obstacles. In urban terrain, object size and composition can vary drastically, from buildings to telephone poles to thin wires and clothes lines. In particular, sparse objects such as trees and bushes are troublesome to detect and avoid.

The UAV will also encounter a variety of environmental and weather conditions. Lighting conditions are often unstructured and unpredictable. The vehicle could move from the shade of a building to direct sunlight in fractions of a second. Smoke from fires or dust from down-wash can blind a UAVs sensor suite. Environmental factors such as rain and fog can further hinder performance. Providing a sensor suite that meets these criteria is essential to fully leveraging the capability of UAVs in near-Earth environments.

As an FCS One Team member, our experiences in sensor suite design revealed that scanning laser range finders are the best suited sensor for performing obstacle detection and collision avoidance. Preliminary experiments against the criteria stated above showed them to out perform common sensors such as sonar, computer vision and optic flow.

The biggest attraction of these sensors is their high fidelity and wide field of view. Their range is comparable if not better than many traditional sensors. Laser range finders are also able to clearly detect many different objects including sparse

1-4244-0912-8/07/$25.00 ©2007 IEEE.

objects. Additionally, they are robust to varied lighting conditions, encountering difficulties only in extreme conditions such as direct sunlight measuring over 10,000 lux.

The major drawback to laser range finders is their sensitivity to obscurants present in the air. Rain can cause reflections that appear to be thin obstacles. Particulate matter such as fog, smoke and dust diffuse the laser beam, making some obstacles undetectable. This detriment can hinder the operational capabilities of the UAV.

Current applications have demonstrated the effectiveness of UAVs in relatively "clear skies". Search and rescue operations supporting hurricane Katrina disaster relief were performed during good weather after the hurricane had passed [2]. Similarly, the mapping of the 2006 Esperanza fire in California was executed by UAVs flying at 43,000 ft. high above the smoke plume [3]. While the role these UAVs played was instrumental in aiding the mitigation effort, our interest is in providing first responders with UAVs that can be deployed in the harsh environments they encounter. For UAVs to perform obstacle detection in real world scenarios, the problem of handling obscurants must be addressed.

Previous work has demonstrated the use of scanning laser range finders for obstacle detection in the absence of obscurants. In [4], a laser range finder mounted to a ground based robot was used to map the inside of a museum and subsequently perform path planning. Their use was also demonstrated outdoors during the DARPA Grand Challenge. Both [5] and [6] show how scanning laser range finders can be used to guide an autonomous ground robot through the desert. For aerial robots, [7] shows the use of laser range finders for terrain mapping and pose estimation. Likewise, [8] shows the use of laser scanners to perform mapping for guiding helicopters through near Earth environments at high speeds. None of these included modeling for obscurants.

Extensive work has been done to model the effect of obscurants. [9] presents a model for the effect of different kinds of smoke and various other obscurants. Such models can be used to correct for obscurants in laser range measurements. However, there has been relatively little work towards modeling and correcting for these effects in simultaneous localization and mapping (SLAM) problems.

This paper examines the effects of obscurants on mapping with SLAM techniques. A Hokuyo laser range finder is characterized for varying rain and fog conditions. The sensor model with and without obscurants was determined from these experiments. Measurements were then taken inside a UAV testing facility. The sensor was scanned through a mock urban environment to mimic flight through cluttered terrain. Inside the test space, environmental disturbances were introduced in a controlled fashion. Specific rain flow rates and fog densities were generated to determine the effect on 3D mapping. A SLAM technique was employed to recover the map under these noisy conditions. The robustness of this technique was tested versus the presence of obscurants.

Section II describes SISTR, a Systems Integrated Sensor Test Rig. Section III discusses how the sensor model is characterized for varying fog and rain conditions. The SLAM algorithm utilized is presented in section IV. The results of applying the SLAM algorithm under obscured conditions are shown in section V. Conclusions are drawn in section VI. Finally, future work is discussed in section VII.

Fig. 2. Rain machine utilized for sensor testing. The machine can generate an 8ft wide by 2ft deep by 10ft tall sheet of rain with flow rates up to .2 in/min.

II. SISTR

Assessment of the laser range finder's performance in disaster scenarios required a testing facility capable of repeatably and controllably simulating realistic disaster environments. SISTR, shown in Fig. 1, is a National Science Foundation funded UAV testing facility that provides this capability. SISTR contains a mock urban environment constructed at full scale with actual materials such as plywood, brick and cinder blocks. The environment can be augmented and reconfigured with other features such as poles, wires and trees to test robustness to varying obstacles.

As described in [10], the facility is surrounded by a six degree-of-freedom computer controlled gantry. Using the math model that describes the flight dynamics of an aircraft, the gantry can be programmed to mimic the flight of a slow flying vehicle. UAVs and UAV sensor suites can be attached to the end effector of the gantry to provide real-time sensor feedback for testing obstacle detection and collision avoidance algorithms.

One unique quality of SISTR is its ability to simulate weather conditions and other disturbances. With test rigs constructed inside the facility, sunlight, rain, fog and other effects can be generated in a controlled, repeatable manner. When determining what conditions to simulate and what standards to test UAVs against, we turned to the US military

Fig. 3. The Hokuyo URG-04LX used for testing. Its small size (50mm x 50mm x 70mm) and light weight (160g) make it an attractive sensor for aerial platforms.

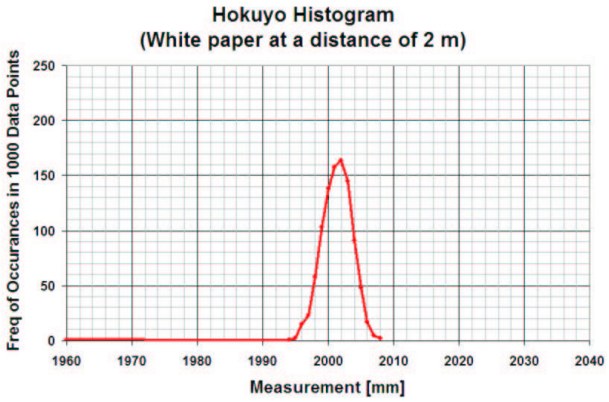

Fig. 4. Histogram showing the range of measurements recorded for a white piece of paper fixed 2m from the sensor. The plot shows the majority of the points occurring at the correct measurement and varying no more than $\pm 1\%$.

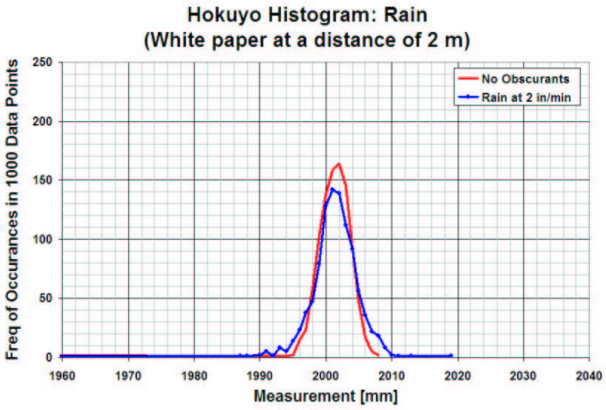

Fig. 5. Histogram showing the effect of rain on sensor measurements. The red line shows measurements without rain, the blue line shows data taken with rain at a rate of .2 in/min.

standards for all weather performance [11]. All military vehicles are held to these standards, including UAVs.

Using this standard as a guide, a custom built rain machine shown in fig. 2 was constructed. This machine can be used to produce a "sheet" of rain 8ft wide by 2ft deep by 10ft tall. This sheet of rain can be introduced between the sensor and the visible field. The sensor therefore looks through the sheet of rain when taking measurements.

Per military spec, the machine was designed to generate flow rates between .011 in/min and .2 in/min with drop diameters of approximately 1mm - 3mm. This allows simulation of conditions from a light drizzle to a heavy downpour.

The effect of fog was simulated using an American DJ Fogstorm 700 fog machine. The simulated fog was not pure water vapor, but rather a mix of water vapor, glycol, and other inert ingredients. However, as suggested in [9] the particle size plays a major role in dispersing light. It is therefore assumed that the principle effect was still effectively modeled by this substance. This infrastructure provides a solid basis for determining the sensor model in the presence of obscurants.

III. CHARACTERIZATION

To account for obscurants in a SLAM implementation, the model of the sensor with obscurants must first be obtained.

A. The Hokuyo

The sensor used for testing was the Hokuyo URG-04LX show in Fig. 3. The biggest draw of this particular sensor is its small form factor. At 50mm x 50mm x 70mm and weighing only 160g, it is one of the smallest scanning laser range finders available. This makes the sensor attractive for small UAVs that fly in near-Earth environments.

According to the manufacturer, the Hokuyo has a range of 20 mm - 4000 mm with an accuracy of $\pm 1\%$ and a 240° field of view with $.36^\circ$ resolution. This detection range is catered towards slow flying aircraft [1]. For example, a craft flying at 4 m/s at best would have 1 sec to react to a detected obstacle. For faster, higher altitude missions, a sensor with a longer range would be required. Since the principle behind all LIDAR sensors is the reflection of light off objects, the results presented herein can be extended to similar sensors.

To confirm the manufacturer's specifications, the sensor was tested under standard environmental conditions. A sheet of white paper was placed 2m from the sensor aligned at 0° (in the middle of the sensing range). 1000 data points were recorded and the resulting histogram plotted in Fig. 4. As can be seen in the figure, the data points were centered around 2000 mm with a standard distribution. This baseline data confirms the specifications, with the majority of the points falling within $\pm 1\%$ of the nominal value.

From this data a probabilistic model of the sensor can be formed. Following standard SLAM procedure, the sensor is modeled as a covariance matrix. In this case it is assumed that the covariance matrix is constant for all scan beams (i.e. for the entire visible range of the sensor). The covariance matrix is then one dimensional, and in the case of no obscurants was found to be $B_o = 5$.

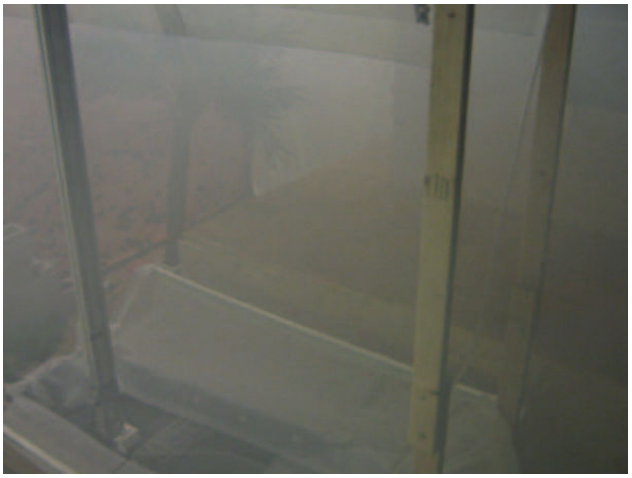

Fig. 6. Image depicting fog density. The fog shown in this condition reduced visibility to approximately 8m.

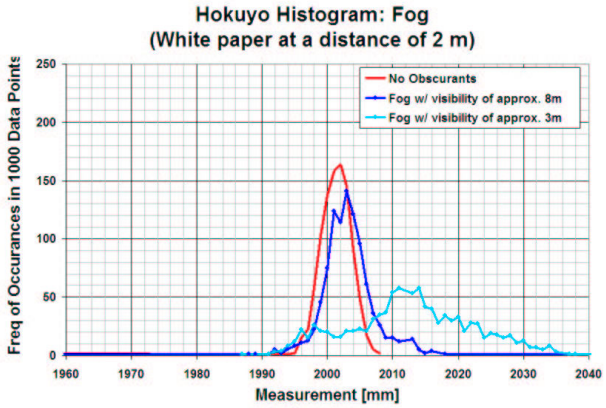

Fig. 7. Histogram showing the effect of fog on sensor measurements. The red line shows measurements without fog, the blue lines show data taken with varying densities of fog.

B. Rain Testing

The rain machine was utilized to test the sensor's performance in rain. Preliminary testing indicated that the most pronounced effect occurred in downpour conditions. Therefore, results were only gathered for the highest flow rate of .2 in/min.

Fig. 5 shows a histogram of the rain data compared to no obscurants measurements. Rain slightly increased the measurement error, thereby slightly increasing the standard deviation. For rain, the covariance matrix on average was found to be $B_{rain} = 8.39$. This shows significant increase over the case with no obscurants.

C. Fog Testing

Fog showed a much more dramatic effect on sensor measurements as seen in Fig. 7. The accuracy of measurements clearly decreases with density of fog. In the heaviest fog, the mean of the distribution has been shifted and the deviation is clearly very large. Since different fog densities had different effects on measurements, there are several models that could be used to approximate laser measurements in fog. For this paper, the fog modeled reduced visibility to approximately 8m, shown in Fig. 6. The covariance matrix in the case of fog in this case was $B_{fog} = 13.75$.

These models of the sensor's performance characterize how the sensor reacts under different environmental conditions. This enables the use of SLAM techniques for extracting maps from obscured sensor data.

IV. SLAM ALGORITHM

The algorithm utilized is a simplified implementation of that presented in [7]. The implementation in [7] corrects for pose error in all 6 dimensions and matches scan points between scans. The implementation utilized in this paper only considers the 3 translational dimensions and assumes scan points match with their predecessor from the previous scan. The fundamental concepts and their application are presented here in brief.

This algorithm produces a 3D map of the environment given noisy pose and terrain measurements. To find the corrected pose, a probabilistic model is constructed. This model is comprised of: the probability of the pose measurement, the probability of differential pose measurements, and the probability of consecutive scan alignment.

The probability of pose measurement is modeled as the probability of measuring the pose given the corrected pose. The system is taken to be 3 degrees of freedom, namely the 3 Cartesian coordinates. Their measurement at the current time step is the vector y_t, while the algorithm solves for the corrected pose x_t. Given the measurement covariance A, the probability of y_t given x_t as presented in [7] is then:

$$p(y_t|x_t) \propto \exp -\frac{1}{2}(y_t - x_t)^T A^{-1}(y_t - x_t) \qquad (1)$$

The method also utilizes a differential model. Typically, the sensors onboard an aircraft measure rotational and translational rates. The pose is recovered through integration, making it susceptible to drift. The differential model is less affected by this error. Given D, the covariance of differential measurements, the differential model as derived in [7] is:

$$p(\Delta y_t|\Delta x_t) \propto \exp -\frac{1}{2}(\Delta y_t - \Delta x_t)^T D^{-1}(\Delta y_t - \Delta x_t) \quad (2)$$

where $\Delta y_t = y_t - y_{t-1}$ and $\Delta x_t = x_t - x_{t-1}$. As differential measurements are more accurate than absolute measurements, the covariance matrix D should represent a Gaussian with smaller standard deviation than A.

The final portion of the model is a representation of the likelihood of a scan. Rather than representing individual features as states as in traditional SLAM, the implementation in [7] models the consistency between consecutive scans as:

$$p(z_t|x_t, x_{t-1}, z_{t-1})$$
$$\propto \prod_i \exp -\tfrac{1}{2} \min[\alpha, \min_j (z_t^i - f(z_{t-1}^j, x_{t-1}, x_t))^T$$
$$B^{-1}(z_t^i - f(z_{t-1}^j, x_{t-1}, x_t))]$$

The goal of this model is to match points from the current scan with points from the previous scan. A point in the

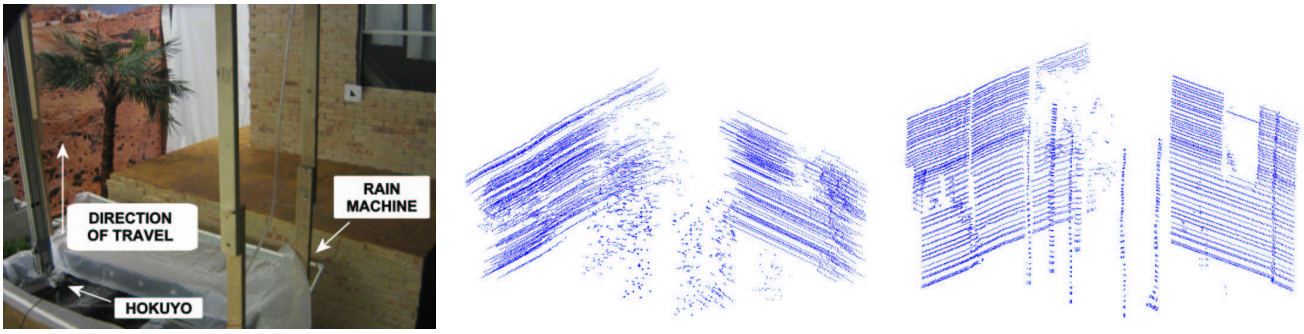

Fig. 8. Results from applying the SLAM algorithm to a data set gathered inside a mock urban environment (left). Gaussian noise was added to the pose measurement to simulate data gathered from a helicopter (center). This data was then used to reconstruct the map (right).

current scan z_t^i is compared to all points from the previous scan z_{t-1}. The function f maps a point from the previous scan z_{t-1}^j into the local coordinate system of the current scan z_t. The inner minimization identifies a point from the previous scan that is closest to the point from the current scan. The outer minimization thresholds this alignment to allow for local inconsistencies such as those from sparse objects. The matrix B is the measurement covariance.

Equations 1, 2 and 3 can be combined to form the probabilistic model for the entire problem [7]:

$$p(y_t|x_t)p(\Delta y_t|\Delta x_t)p(z_t|x_t, x_{t-1}, z_{t-1}) \tag{3}$$

The map and pose are recovered by finding the pose that maximizes this likelihood, or by minimizing the negative log likelihood given by [7]:

$$\begin{aligned} const + \frac{1}{2}((y_t - x_t)^T A^{-1}(y_t - x_t) \\ +(\Delta y_t - \Delta x_t)^T D^{-1}(\Delta y_t - \Delta x_t) \\ + \sum_i \min[\alpha, \min_j (z_t^i - f(z_{t-1}^j, x_{t-1}, x_t))^T \\ B^{-1}(z_t^i - f(z_{t-1}^j, x_{t-1}, x_t))]) \end{aligned}$$

This minimization is found by first minimizing to align the current scan with the previous scan, and then performing hill-climbing to determine the pose that minimizes the negative log likelihood. These steps can be iterated until the negative log likelihood falls within a threshold.

This algorithm was applied to a data set gathered with no obscurants. The Hokuyo was attached to the end effector of a gantry. The gantry was capable of translating the Hokuyo through a mock urban environment, simulating the flight of a UAV through cluttered terrain. In this case, the Hokuyo was moved vertically upwards from the floor towards the ceiling as depicted in Fig. 8. The gantry provided X, Y and Z measurements of the pose while the Hokuyo provided scan data of the environment. To simulate noise on the pose sensors, Gaussian noise was added to the pose measurement.

The results are shown in Fig. 8. The image on the left shows the environment that was scanned. The Hokuyo is mounted to the end of the gantry, oriented such that it captures the building in front of it, the rain machine, and the palm tree. The plot in the center shows the resulting map with Gaussian noise added, typical of raw data gathered from a UAV platform. The plot on the right shows the same data after being processed by the SLAM algorithm. The results show the ability of the algorithm to recover the map from noisy pose measurements. What remains to be seen is the robustness of the algorithm to noisy laser scans.

V. Results

The sensor models acquired earlier were utilized in equation 3 to form a model of the UAV in the presence of obscurants. The SLAM algorithm was then applied to terrain scans acquired under rainy and foggy conditions.

Fig. 9 shows the results of applying the algorithm to terrain scans acquired in the presence of rain with a flow rate of 2 in/min. As can be seen in the figure, the rain had little effect on the resulting map. The algorithm successfully recovered the terrain with little to no noise present in the 3D plot.

Fig. 10 shows the results of applying the algorithm to terrain scans acquired in the presence of fog with a visibility of approximately 8m. Again, the algorithm successfully recovered the map. However, the effect of sensor noise is much more evident. The resulting map is uneven in several places. It should also be noticed that some features were lost. In particular, the tree is not as defined as in fig. 8.

Finally, fig. 11 shows the results of applying the algorithm to terrain scans acquired in the presence of fog with a visibility of approximately 2m. Under such extreme conditions, there were several scans that were unable to penetrate the fog. This drastically effected the resulting 3D plot. Major features such as the building were lost at points, replaced by a cloud of noise that surrounds the sensor.

VI. Conclusions

The results show that in general the algorithm is robust to obscurants. The rain conditions showed little effect on sensor measurements. While these results are accurate, it is believed that the effect would be more pronounced had the rain been distributed over a larger volume. Further testing is necessary to fully characterize this condition.

The Hokuyo is surprisingly robust to fog. Only under the most extreme conditions did the Hokuyo - and subsequently

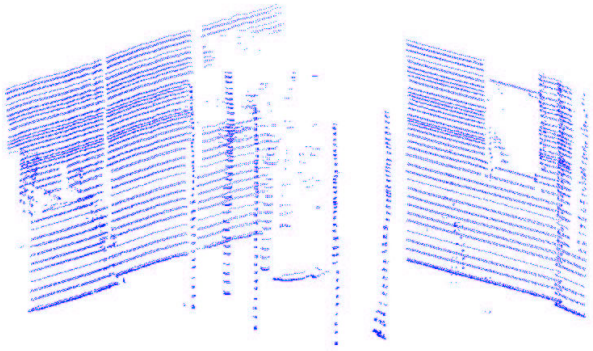

Fig. 9. 3D point cloud of the mock urban environment showing the results of applying the SLAM algorithm under rainy conditions with a flow rate of 2 in/min. The rain had little effect on the map.

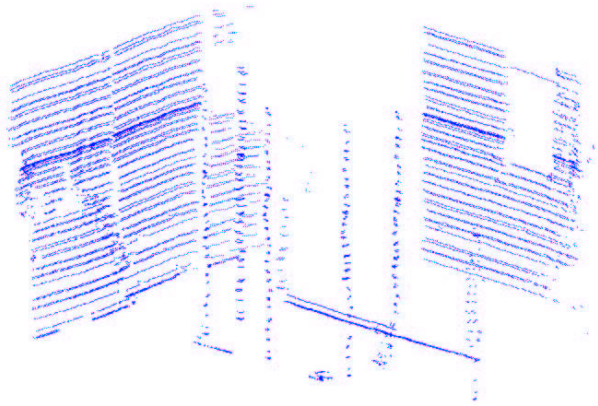

Fig. 10. 3D point cloud of the mock urban environment showing the results of applying the SLAM algorithm under foggy conditions with visibility of approximately 8m. The SLAM algorithm performed well, though some features were lost (such as the tree).

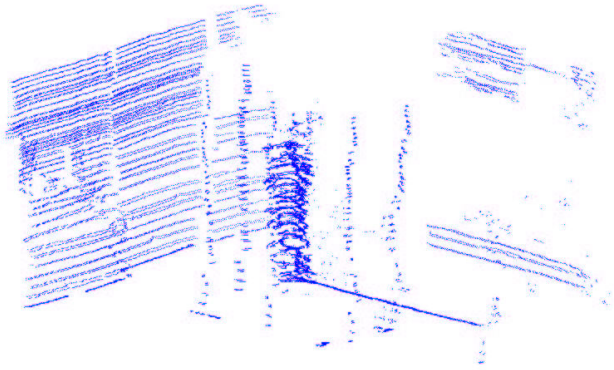

Fig. 11. 3D point cloud of the mock urban environment showing the results of applying the SLAM algorithm under foggy conditions with visibility of approximately 3m. Under such extreme conditions, there were scans which contained no terrain information. This drastically effected the resulting map.

the SLAM algorithm - fail. However, the results do clearly show that the noise from fog results in uneven maps. Also, objects that are more difficult to detect (such as the leaves on the tree) are lost in foggy conditions. This result could prove useful in path planning and collision avoidance algorithms for UAVs. If the UAV is able to ascertain that foggy conditions are present, it could be instructed to proceed with caution, especially in areas with trees or bushes.

VII. FUTURE WORK

The results presented in this paper demonstrate the ability to detect and map terrain features in the presence of obscurants. However, it was shown that fog introduces noise to the map and causes some features to be lost. The current algorithm adjusts the pose measurement, but does not correct scan data. The algorithm could be modified to filter sensor data to produce more consistent maps in obscured conditions. This would come at the expense of processing time.

Also, the algorithm fails when the laser range finder is blinded. This could prove detrimental to the craft. To mitigate this condition, work needs to be done to investigate deriving terrain from previous "good" scans or fusing data from other sensors onboard that are not as affected by obscurants.

REFERENCES

[1] W. Green, P. Oh, and G. Barrows "Flying Insect Inspired Vision for Autonomous Aerial Robot Maneuvers in Near-Earth Environments", *Int. Conf. on Robotics and Automation (ICRA)*, New Orleans, LA, pp. 2347-2352, April 2004.

[2] R. Murphy, C. Griffin, S. Stover, and K. Pratt, "Use of Micro Air Vehicles at Hurricane Katrina", *IEEE Workshop on Safety Security Rescue Robots*, Gaithersburg, MD, 2006.

[3] NASA Dryden (November 6, 2006). NASA Supports UAS Fire Mapping Efforts on California Fire. Press Release.

[4] S. Thrun et. al. "Probabilistic algorithms and the interactive museum tour-guide robot Minerva". *Int. Journal of Robotics Research*, vol. 19, no. 11, pp. 972-999, Nov. 2000.

[5] S. Thrun et. al., "Stanley, The Robot That Won the Darpa Grand Challenge", *Journal of Field Robotics*, vol. 23, no. 9, pp. 661-692, Sept. 2006.

[6] W. Whittaker et. al, 2006. "A Robust Approach to High-Speed Navigation for Unrehearsed Desert Terrain", *Journal of Field Robotics*, vol. 23, no. 8, pp. 467-508, Aug. 2006.

[7] S. Thrun, M. Diel, D. Hahnel, "Scan Alignment and 3-D Surface Modeling with a Helicopter Platform", *The 4th Int. Conf. on Field and Service Robotics*, Lake Yamanaka, Japan, pp. 14-16, July 2003.

[8] S. Scherer, S. Singh, L.J. Chamberlain, and S. Saripalli, "Flying Fast and Low Among Obstacles", *Int. Conf. on Robotics and Automation*, Roma, Italy, pp. 2023-2029, April 2007.

[9] A. Dimmeler, D. Clement, W. Biichtemann, "Effects of Obscurants on the Performance of Laser Range Finders", FGAN-FfO, Tubingen, Germany, Tech. Rep. FGAN-FfO 1998/6.

[10] V. Narli, P. Oh, "A Hardware-in-the-Loop Test Rig for Designing Near-Earth Aerial Robotics", *Int. Conf. on Robotics and Automation (ICRA)*, Orlando FL, pp. 2509-2514, May 2006.

[11] Army Regulation 70-38, "Research, Development, Test And Evaluation Of Materiel For Extreme Climatic Conditions", 15 Sept, 1979.